Wencka et al. Journal of Analytical Science and Technology (2018) 9:12
https://doi.org/10.1186/s40543-018-0144-2

Journal of Analytical Science and Technology

RESEARCH ARTICLE Open Access

The effect of surface oxidation on the catalytic properties of Ga_3Ni_2 intermetallic compound for carbon dioxide reduction

Magdalena Wencka[1], Janez Kovač[2], Venkata D. B. C. Dasireddy[3], Blaž Likozar[3], Andreja Jelen[2], Stanislav Vrtnik[2], Peter Gille[4], Hae Jin Kim[5] and Janez Dolinšek[2,6*]

Abstract

Background: In a routine handling of a catalyst material, exposure to air can usually not be avoided. For noble metal catalysts that are resistant to oxidation, this is not an issue, but becomes important for intermetallic catalysts composed of two or more non-noble chemical elements that possess much different standard enthalpies of the oxide formation. The element with higher affinity to oxygen concentrates on the surface in the oxide form, whereas the element with lower affinity sinks into the subsurface region. This changes the number of active sites and the catalytic performance of the catalyst. We have investigated the instability of the surface composition to oxidation of the Ga_3Ni_2 noble metal-free intermetallic compound, a new catalyst for the CO_2 reduction to CO, CH_4 and methanol.

Methods: The instability of the oxidized Ga_3Ni_2 surface composition to different heating–annealing conditions was studied by X-ray photoelectron spectroscopy (XPS), used to determine the elemental composition and the chemical bonding in the near-surface region. The dispersion of active sites available for the chemisorption of H_2 and CO on the Ga_3Ni_2 catalyst surface was determined by H_2 and CO temperature-programmed desorption. CO_2 conversion experiments were performed by using the catalyst material reduced in hydrogen at temperatures of 300 and 600 °C.

Results: XPS study of the Ga_3Ni_2 surface subjected to different heating–annealing conditions has revealed that the concentration of Ga at the oxidized surface is strongly enhanced and the concentration of Ni is strongly depleted with respect to the values in the bulk. By annealing the surface at 600 °C in ultra-high vacuum, the oxides have evaporated and thermal diffusion of atoms near the surface has partially reconstructed the surface composition towards the energetically more favorable bulk value, whereas annealing at a lower temperature of 300 °C was ineffective to change the surface composition. Catalytic tests were in agreement with the XPS results, where an increased CO_2 conversion for the catalyst reduced with hydrogen at a higher temperature followed an increased Ni/Ga surface concentration ratio.

Conclusions: The instability of the active surface chemical composition to oxidation in air must be taken into account when considering noble metal-free intermetallic catalysts as alternatives to the conventional catalysts based on noble metals. Ga_3Ni_2 and other Ga–Ni intermetallic compounds are good examples of binary intermetallic catalysts, whose catalytic performance is strongly affected by exposure to the air.

Keywords: Ga_3Ni_2 intermetallic catalyst, Surface instability to oxidation, CO_2 catalytic conversion

* Correspondence: jani.dolinsek@ijs.si
[2]Jožef Stefan Institute, Jamova 39, 1000 Ljubljana, Slovenia
[6]Faculty of Mathematics and Physics, University of Ljubljana, Jadranska 19, 1000 Ljubljana, Slovenia
Full list of author information is available at the end of the article

Background

Intermetallic compounds were proven to be attractive alternatives to pure and alloyed metals as catalyst materials in heterogeneous catalysis because of their increased selectivity to specific reactions and better long-term stability (Armbrüster et al. 2014). Intermetallic compounds can be reproducibly prepared in a controlled manner, and their ordered crystal structures imply that the number of catalytically active sites and the distances between them are well defined and uniformly repeat over the crystal. By selecting intermetallic compounds with suitable crystal structures and chemical elements, the active sites can be tailored to the needs of a particular chemical reaction (Armbrüster et al. 2011). Fixed crystal structures do not allow clustering of the catalytically active atoms during operation of the catalyst, which is a decisive difference to alloys.

Palladium-based intermetallic compounds M_mPd_n with M = Ga or In (including GaPd, $GaPd_2$, Ga_7Pd_3, and InPd) were proven to be highly selective and stable catalyst materials for the selective hydrogenation of alkynes and the methanol steam reforming reaction (Armbrüster et al. 2010, 2011, 2014; Kovnir et al. 2007; Osswald et al. 2008; Klanjšek et al. 2012; Wencka et al. 2014, 2015). For the industrial heterogeneous catalysis processes, it is advantageous to replace precious metals by less expensive alternatives. In such an attempt, the intermetallic $Al_{13}Fe_4$ was found to be an excellent replacement for palladium in the heterogeneous hydrogenation of alkynes (Armbrüster et al. 2012). Another precious metal (and noble metal)-free series of intermetallic catalysts were discovered in the Ga–Ni system (GaNi, $GaNi_3$, Ga_3Ni_5), which reduce CO_2 to methanol at ambient pressure (Studt et al. 2014; Sharafutdinov et al. 2014).

In a routine handling of the catalyst material, exposure to air can usually not be avoided. For noble metal catalysts (Pt, Pd, Au, Ag, Cu, …) that are resistant to corrosion and oxidation in moist air, exposure to air is not an important issue, but it becomes essential for noble metal-free intermetallic catalysts composed of two or more chemical elements that possess much different standard enthalpies of the oxide formation. The element with higher affinity to oxygen (more negative standard enthalpy of formation) will concentrate on the surface in the oxide form, whereas the element with lower affinity will sink into the subsurface region. The surface chemical composition may thus be strongly altered with respect to the bulk one, which affects the number of active sites. Surface reduction with hydrogen gas just prior to the catalytic runs cleans the oxides, but the oxide-free surface composition remains altered. Upon heating the clean catalyst in an atmosphere that does not contain oxygen, thermal diffusion of atoms near the surface tends to restore the surface stoichiometry towards the energetically more favorable bulk value, but the degree of restoration depends on the temperature and the time spent at high temperature. The number of active sites, their geometric distribution on the surface, and the consequent catalytic activity and selectivity will thus depend on the heating–annealing conditions.

In this work, the instability of the active surface chemical composition to oxidation in air was studied for the Ga_3Ni_2 intermetallic catalyst, belonging to the nickel-poor side of the Ga–Ni phase diagram (Okamoto 2010) that has not been investigated previously. Ga_3Ni_2 is the only compound in the Ga–Ni system that is in equilibrium with the binary Ga–Ni melt, so growth of single crystals is possible. Though single crystals are not used in catalytic applications, they are advantageous to prepare well-defined crystalline surfaces along specific crystallographic planes for fundamental surface studies related to catalysis. In addition, phase purity of a single-crystalline sample is usually superior to that of a polygrain material, so crushing a single crystal into powder provides phase-pure catalyst material. Our Ga_3Ni_2 powder catalyst material was prepared by crushing a single crystal grown by the Czochralski technique (Wencka et al. 2016). We have tested the effect of oxidation on the catalytic performance of Ga_3Ni_2 in hydrogenation reactions that reduce CO_2 to CO, CH_4, and methanol, by varying heating–annealing conditions that alter the surface chemical composition and the consequent catalytic performance. Oxidation has happened during crushing the Ga_3Ni_2 single crystal into powder under ambient conditions prior to the catalytic testing. The foundation hydrogenation reactions are given below:

$H_2 + CO_2 \leftrightarrow CO + H_2O$ (reverse water–gas shift reaction (rWGS))

$4H_2 + CO_2 \leftrightarrow CH_4 + 2H_2O$ (methanation)

$3H_2 + CO_2 \leftrightarrow CH_3OH + H_2O$ (methanol synthesis)

On the microscopic level, the instability of the oxidized Ga_3Ni_2 surface composition to different heating–annealing conditions was studied by X-ray photoelectron spectroscopy (XPS), used to determine the elemental composition and the chemical bonding in the near-surface region. The XPS depth profiling technique was applied to the oxidized monocrystalline surface at temperatures between 25 and 600 °C in ultra-high vacuum (UHV) and in the presence of a diluted H_2 atmosphere.

Methods

Ga_3Ni_2 crystallizes in the Al_3Ni_2-type structure (Hellner and Laves 1947), trigonal space group $P\bar{3}m1$, and lattice parameters $a = 0.405$ nm and $c = 0.489$ nm (Wencka et al. 2016). The trigonal unit cell is shown in Fig. 1. The X-ray diffraction (XRD) pattern of the employed Ga_3Ni_2

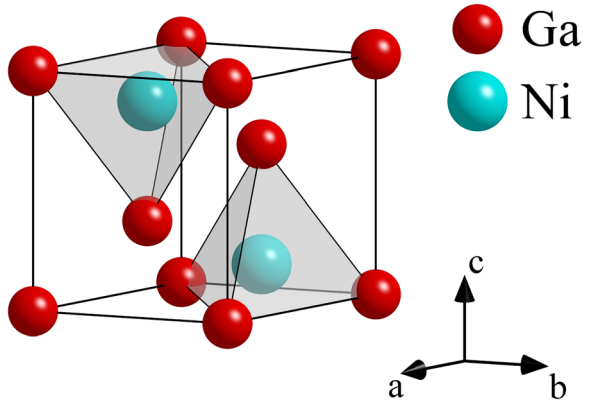

Fig. 1 The Ga_3Ni_2 trigonal unit cell (Wencka et al. 2016; Hellner and Laves 1947)

single crystal grown by the Czochralski technique is shown in Wencka et al. 2016, demonstrating high degree of structural order and phase purity. Its decomposition temperature was determined by differential thermal analysis (DTA) (Wencka et al. 2016). Upon heating, there is an onset of a pre-peak at 934 °C and the main endothermic peak at 948 °C, whereas no thermal effects were observed at lower temperatures. The main peak corresponds well to the phase diagram (Okamoto 2010), which shows the peritectic temperature of Ga_3Ni_2 at 950 °C. The onset of a step at temperatures lower than that of a peritectic decomposition (here at 934 °C) is typical of solution-grown crystals that have been grown at tunable temperatures below the peritectic one. Upon DTA cooling, the peritectic back-reaction starts at the same temperature of 948 °C and there is almost no undercooling effect. The Ga_3Ni_2 crystal is thus stable up to these high temperatures.

The distribution of particles' cross dimensions in the metallic powder obtained by crushing a piece of the single crystal was determined from SEM backscattered electron images (not shown), where 95% of the particles were in the range 50 nm–5 μm. The specific surface area of the catalyst determined by the single-point Brunauer–Emmett–Teller (BET) method using nitrogen as the probe molecule was found to amount to 0.8 m^2/g. This relatively small specific surface is a consequence of the small surface–to–volume ratio of the powder obtained by crushing a crystal.

The dispersion of active sites available for the chemisorption of H_2 and CO on the Ga_3Ni_2 catalyst surface was studied by H_2 and CO desorption experiments. Temperature-programmed desorption (TPD) runs were carried out using the Micrometrics 2920 Autochem II Chemisorption Analyzer. In a TPD analysis, the catalyst is first reduced by hydrogen to activate the surface (the same procedure is applied before the catalytic tests). Prior to the reduction, the catalyst was pre-treated by heating in a stream of argon (30 mL min^{-1}) at 400 °C for 30 min in order to remove physisorbed gases on the surface. Thereafter, 4.9 mol% hydrogen in argon was used as the reducing agent at the flow rate of 30 mL min^{-1} and the temperature was raised from 25 to 600 °C using the ramp rate of 10 °C min^{-1}. After the reduction, the temperature was decreased to 80 °C. In the subsequent TPD experiments, an appropriate gaseous mixture was passed over the catalyst (4.9 mol% H_2 in Ar for H_2–TPD and 10 mol% CO in He for CO–TPD) at the flow rate of 30 mL min^{-1}. The excess gas was removed by purging with helium for 30 min. The temperature was consequently gradually raised to 650 °C by ramping at 10 K min^{-1} under the flow of helium, and the desorption data of H_2 and CO were recorded. The signals from the thermal conductivity detector (TCD) were calibrated using various gas mixtures of H_2 and CO. The above described H_2–TPD and CO–TPD experiments were repeated also for the catalyst reduced at a lower temperature of 300 °C.

Catalytic conversion runs were carried out in a vertical fixed-bed U-shaped quartz reactor (100 cm length and 1.5 cm internal diameter). Electric furnace fitted with a temperature-programmed controller heated the reactor, and the temperature of the reactor was monitored using a type K thermocouple. The flow rates of the gases were measured and controlled by Brooks mass flow meters. The Ga_3Ni_2 catalyst (0.1 g) was placed in the intermediate section of the reactor. The reaction mixture consisted of CO_2:H_2 molar ratio 1:1, and the gas hourly space velocity (GHSV) of the reaction was maintained at 60,000 h^{-1}.

XPS surface analysis was performed by using a TFA XPS instrument (Physical Electronics Inc.) equipped with an Al-monochromatic X-ray source ($E = 1486$ eV). The XPS-analyzed volume was 0.4 mm in diameter and 3–5 nm in depth. The XPS carbon C 1s signal at 284.8 eV measured at the surface was used to calibrate the binding energy scale of the XPS spectra due to possible shift of the spectra related to sample charging.

Results

Catalyst characterization

The results of the TPD analysis are summarized in Table 1, where the amounts of released H_2 and CO per gram of the Ga_3Ni_2 catalyst reduced at two different temperatures of 300 or 600 °C, respectively, are given. The catalyst reduced at a higher temperature of 600 °C showed a factor ~ 1.8 larger hydrogen coverage of the surface as compared to the catalyst reduced at a lower temperature of 300 °C. Higher reduction temperature has also increased the CO adsorption by about the same factor (~ 1.7). The H_2–TPD data were used to calculate

Table 1 Metal dispersion D, the amounts of released H_2 and CO per gram of the Ga_3Ni_2 catalyst determined from TPD experiments, the reaction rate r_{CO_2}, and the CO_2 turnover frequency (TOF) at 500 °C of the catalyst reduced at two different temperatures of 300 or 600 °C, respectively

Reduction T	D (%)	H_2–TPD (μmol H_2 g^{-1})	CO–TPD (μmol CO g^{-1})	r_{CO_2} at 500 °C (μmol CO_2 g^{-1} s^{-1})	TOF at 500 °C (s^{-1})
300 °C	0.06 ± 0.01	1.8 ± 0.2	0.07 ± 0.01	1.4 ± 0.15	0.42 ± 0.04
600 °C	0.11 ± 0.01	3.2 ± 0.2	0.12 ± 0.01	2.2 ± 0.15	0.39 ± 0.04

the dispersion of active sites D (reported here as metal dispersion) by assuming Ni to be the catalytic species. Metal dispersion was defined as

$$D = \frac{2 \times (\text{no. } H_2 \text{ molecules chemisorbed})}{\text{Total no. of Ni atoms}}, \quad (1)$$

where the Ni:H ratio in the chemisorption was taken as 1. Metal dispersion was found to be rather small for both reduction temperatures, because of the low surface-to-volume ratio of the employed powder material. It has changed from D = 0.06% for the 300 °C-reduced catalyst to D = 0.11% for the 600 °C reduction, an increase by a factor 1.8.

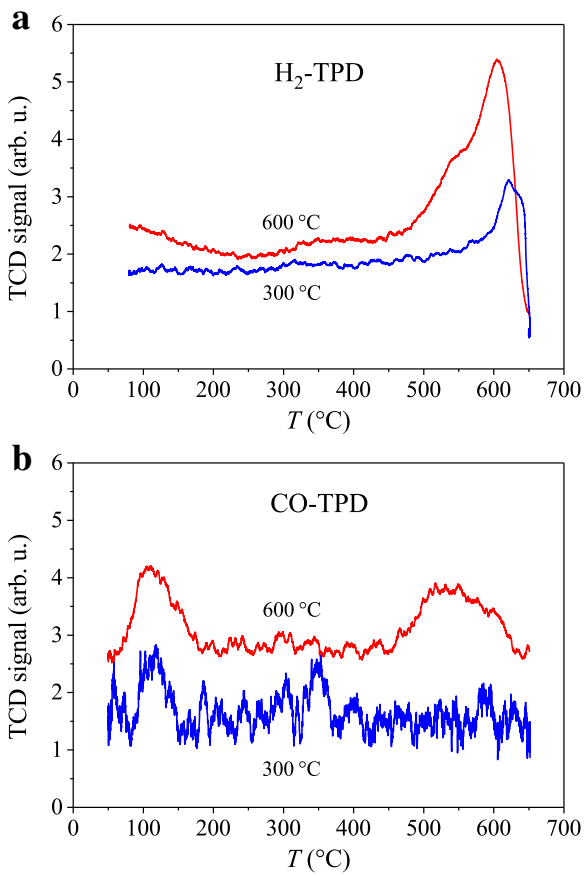

Fig. 2 **a** H_2–TPD and **b** CO–TPD profiles of the Ga_3Ni_2 catalyst reduced at 300 or 600 °C, respectively. Vertical axis shows the signal from the thermal conductivity detector (TCD)

The H_2–TPD and CO–TPD profiles are shown in Fig. 2. The H_2–TPD profile (Fig. 2a) of the catalyst reduced at 600 °C shows a steep increase of the desorbed hydrogen at temperatures above 450 °C with the peak at about 600 °C and a sharp drop at still higher temperatures. The catalyst reduced at 300 °C shows similar peak, but of much lower intensity due to smaller hydrogen coverage of the surface.

The CO–TPD profile (Fig. 2b) of the catalyst reduced at 600 °C shows two distinct peaks, a low-temperature peak centered at about 120 °C and a high-temperature peak centered at about 550 °C. In the CO–TPD profile of the catalyst reduced at 300 °C, these peaks are absent (or there may still be a trace of the low-temperature peak hidden in the noise).

Catalytic testing

Prior to the activity tests, the catalyst was reduced under H_2 for 2 h at 300 or 600 °C, respectively. The CO_2 conversion experiment was conducted in the temperature range between room temperature and 500 °C, and the CO_2 conversion factor X_{CO_2} was calculated from the expression

$$X_{CO_2} = \frac{(\text{moles } CO_2)_{\text{in}} - (\text{moles } CO_2)_{\text{out}}}{(\text{moles } CO_2)_{\text{in}}}. \quad (2)$$

The CO_2 conversion data over the Ga_3Ni_2 catalyst reduced at 300 or 600 °C, respectively, are shown in Fig. 3a. For both reduction temperatures, the onset temperature for the CO_2 conversion was from 100 °C and the maximum conversion was obtained at 500 °C. The conversion was below the equilibrium conversion of the rWGS reaction (black solid curve) (Kim et al. 2012, 2013). The conversion over the catalyst reduced at 600 °C was considerably higher than the conversion over the catalyst reduced at 300 °C, which correlates to the larger metal dispersion of the former that chemisorbs more CO_2 at the surface. Upon completion of the reaction, measurements were taken also on cooling and the results were within the same range as those on heating. We have tested also the bare nickel oxide NiO, which did not show any activity within the temperature range tested (Fig. 3a). We

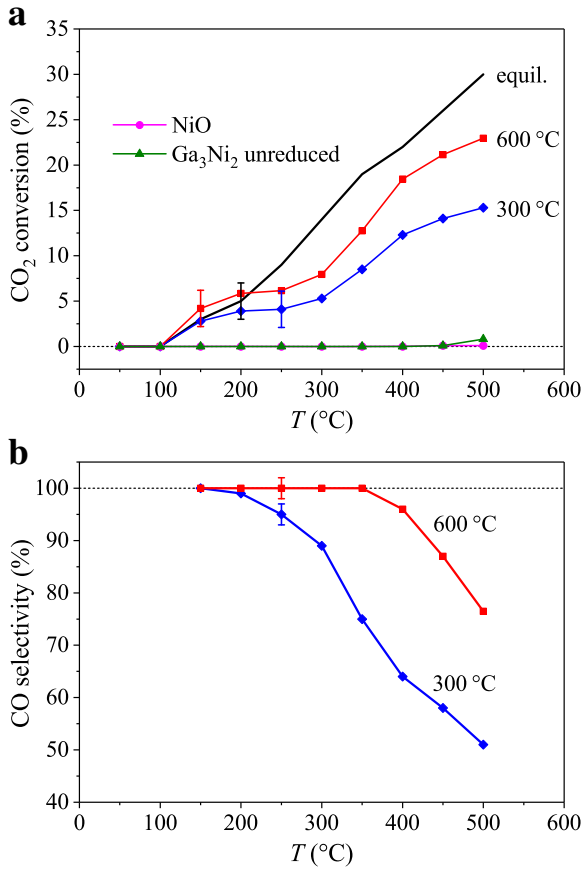

Fig. 3 **a** CO_2 conversion data over the Ga_3Ni_2 catalyst reduced at 300 or 600 °C, respectively (CO_2:H_2 ratio of 1:1, GHSV = 60,000 h^{-1}). The equilibrium conversion of the rWGS reaction is shown by the black solid curve (Kim et al. 2012, 2013). Conversion over the nickel oxide NiO and the unreduced Ga_3Ni_2 was also tested, showing no activity within the investigated temperature range. **b** CO selectivity data over the Ga_3Ni_2 catalyst reduced at 300 or 600 °C, respectively

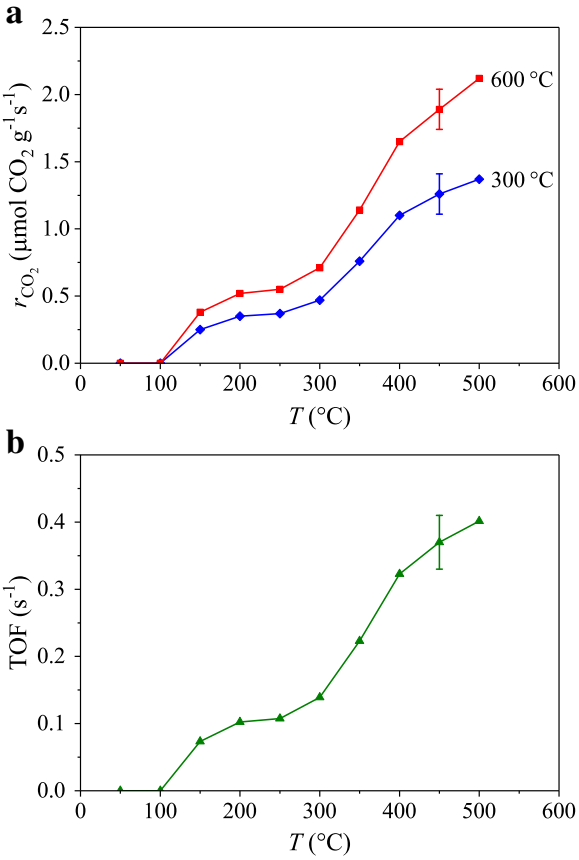

Fig. 4 **a** Reaction rate r_{CO_2} as a function of temperature for the Ga_3Ni_2 catalyst reduced at 300 or 600 °C, respectively. **b** The CO_2 turnover frequency (TOF) as a function of temperature

also tested the unreduced Ga_3Ni_2 catalyst for comparison, which showed no conversion at all.

Reaction rates were measured in separate experiments, in which the conversion of the reactants was maintained below 100% such that differential reaction conditions and negligible heat and mass transfer effects could be assumed. The reaction rate r_{CO_2} (in units mol CO_2 g^{-1} s^{-1}) was calculated from the expression

$$r_{CO_2} = \frac{X_{CO_2} \times F_{CO_2}}{m}, \quad (3)$$

where F_{CO_2} is the CO_2 flow rate (1.35 mL min^{-1}) and m (0.1 g) is the mass of the catalyst. The temperature-dependent reaction rate of the Ga_3Ni_2 catalyst reduced at 300 or 600 °C, respectively, is shown in Fig. 4a. The r_{CO_2} values at the highest investigated temperature of 500 °C are also given in Table 1 for comparison. The 500 °C value r_{CO_2} = 2.2 μmol g^{-1} s^{-1} of the catalyst reduced at 600 °C is by a factor ~ 1.6 larger than r_{CO_2} = 1.4 μmol g^{-1} s^{-1} of the catalyst reduced at 300 °C. The reaction rate expressed in number of CO_2 molecules converted per single metal (Ni) atom per second (the CO_2 turnover frequency (TOF), in units s^{-1}) was determined from the expression

$$\mathrm{TOF} = \frac{X_{CO_2} \times F_{CO_2}}{\text{no. Ni atoms exposed}}, \quad (4)$$

where the CO_2 flow rate is recalculated in number of CO_2 molecules per second (F_{CO_2} = 6.2×10^{17} s^{-1}) and no. Ni atoms exposed = D × Total no. Ni atoms. The TOF values at 500 °C of the catalyst reduced at 300 °C (0.42 ± 0.04 s^{-1}) or 600 °C (0.39 ± 0.04 s^{-1}) are identical within the experimental uncertainty (the values are also given in Table 1). This is a plausible result, indicating that the increased activity of the Ga_3Ni_2 catalyst reduced at 600 °C, as compared to the 300 °C-reduced one, originates from an increased number of active sites (since the metal dispersion D and the reaction rate r_{CO_2} have both

increased by about the same factor of ~ 1.7), whereas the type of active sites (Ni) remains the same (equal TOFs). The temperature-dependent TOF curve (an average of the TOF curves of the catalysts reduced at 300 and 600 °C, respectively) is shown in Fig. 4b.

CO and CH_4 were the only carbon products detected in the outlet gas stream, whereas no methanol has formed. The CO selectivity defined as

$$\text{CO selectivity} = \frac{\text{moles CO}}{\text{moles CO} + \text{moles CH}_4} \quad (5)$$

is shown in Fig. 3b. For both reduction temperatures, only CO was produced at low temperatures. For the catalyst reduced at 300 °C, the 100% CO selectivity was obtained at temperatures below 200 °C, where CO_2 conversion is low, reaching a maximum of 5% only. At higher temperatures, CO formed via the rWGS reaction is converted to methane. The selectivity towards CO consequently decreases with increasing temperature, reaching 50% at the highest investigated temperature of 500 °C. For the catalyst reduced at 600 °C, the range of 100% CO selectivity is extended up to 350 °C, where the CO_2 conversion is already significant, reaching about 13%. At 500 °C, where the CO_2 conversion reaches its maximum value of 22%, the CO selectivity drops to 75%.

XPS surface analysis

XPS gives information on the elemental composition within a thin surface layer of the material (3–5 nm depth in our case) and on the chemical bonding of the elements (oxide, metal). Ar-ion sputtering (4 keV) was used in the XPS depth profiling to remove material with a rate of 2 nm/min, which was calibrated on a flat Ni/Cr multilayer structure of known thickness. Composition depth profile was measured for 25 min, reaching the depth of 50 nm.

The XPS surface analysis was performed on a bulky piece of the Ga_3Ni_2 single crystal that was oxidized due to contact with air. The surface orientation in the Ga_3Ni_2 trigonal crystal system was $(2\bar{1}0)$, i.e., [100] direction was normal to the surface. Elemental composition was determined at temperatures between 25 and 600 °C in either UHV or a diluted H_2 atmosphere. The experiment included the following steps:

1. The first experiment was performed at 25 °C in UHV of 2×10^{-9} mbar on the as-grown oxidized crystal. The resulting XPS elemental concentration depth profile (in at. %) is shown in Fig. 5a. The elements detected were Ga, Ni, O, and C. Carbon contamination was mainly confined to the surface and is excluded from the analysis. The Ni/Ga concentration ratio at the oxidized surface amounted to $R^{surf}_{Ni/Ga} = 0.12 \pm 0.02$. With increasing depth, the oxygen concentration rapidly dropped, whereas the concentrations of Ga and Ni increased and did not change much at depths larger than about 10 nm, where bulk values for the specific crystallographic orientation of the surface were reached ($R^{bulk}_{Ni/Ga} = 0.83 \pm 0.04$). The depth profile of the Ni/Ga concentration ratio is shown in Fig. 5b. Considering the Ga and Ni concentrations within the oxidized surface layer, the surface was strongly enhanced in Ga and depleted in Ni relative to the concentrations in the bulk.

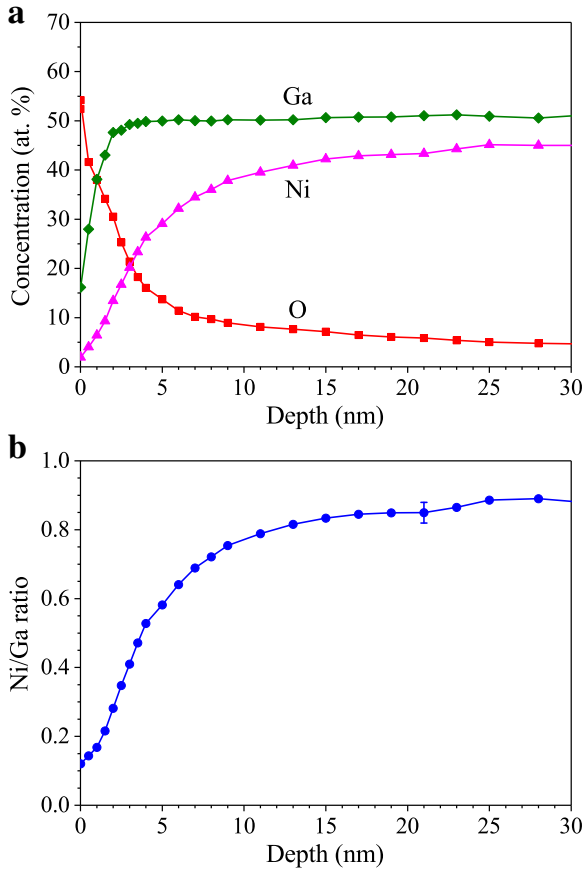

Fig. 5 **a** XPS elemental concentration depth profile (in at. %) at 25 °C of the Ga_3Ni_2 single crystal that was oxidized due to contact with air. **b** The corresponding depth profile of the Ni/Ga concentration ratio

The nonzero oxygen concentration at large depths of the concentration profile shown in Fig. 5a (corresponding to the oxygen signal detected after a long sputtering time) is artificial. During the XPS depth profiling, a relatively large area of the sample (about 0.4 mm in diameter) is analyzed, where the

surface material is removed layer by layer by the Ar-ion sputtering process. Due to surface roughness, some regions are sputtered less effectively, yielding oxygen signal from the surface even after longer sputtering times. Some surface oxygen comes also from the borders of the sputtered region. Since the sputtering time on the abscissa of Fig. 5a was converted into the sputtering depth (with the conversion factor 2 nm/min), these two effects yield an artificial nonzero oxygen concentration at deeper regions of the concentration profile.

2. In the second step, the temperature was raised to 130 °C and the material was kept there for 14 h in UHV for surface degassing. The temperature was then raised to 300 °C and the concentrations of O, Ga, and Ni were measured in the uppermost surface layer (3–5 nm depth) as a function of time for 4 h. For the first 2 h, the sample was kept in UHV, then a diluted H_2 atmosphere was introduced into the XPS chamber (pressure of 4×10^{-7} mbar) and the concentrations were monitored for another 2 h. No change of the oxygen concentration with time was detected, and the Ni/Ga concentration ratio at the surface also remained constant at the value $R^{surf}_{Ni/Ga} = 0.12 \pm 0.02$. The time dependence of $R^{surf}_{Ni/Ga}$ during annealing at 300 °C is shown in Fig. 6a. The surface remained strongly enhanced in Ga and depleted in Ni relative to the bulk concentrations, and the annealing at 300 °C in either UHV or diluted H_2 atmosphere did not change the surface composition.
3. In the third step, the temperature was raised from 300 to 600 °C in 2 h. The concentrations of O, Ga, and Ni were then measured in the surface layer as a function of time for 2.5 h after the 600 °C temperature was set. A diluted H_2 atmosphere was introduced into the XPS chamber 12 min after the concentration measurements have started. The O, Ga, and Ni concentrations as a function of the annealing time are shown in Fig. 6b, whereas the time dependence of the Ni/Ga surface concentration ratio $R^{surf}_{Ni/Ga}$ is presented in Fig. 6c. The oxygen concentration has dropped by a factor of 10 already within the short time period of 12 min before the H_2 introduction (when the sample was still in UHV) and then did not change significantly anymore in the presence of H_2. Within the same time period, $R^{surf}_{Ni/Ga}$ increased strongly from the initial value $R^{surf}_{Ni/Ga} = 0.23 \pm 0.02$ to the value $R^{surf}_{Ni/Ga} = 0.43 \pm 0.03$ that was reached at the moment of the H_2 introduction and then did not change significantly anymore with the annealing time in the presence of H_2. These results indicate that (*i*) the oxides were removed from the surface at 600 °C in the time of about 12 min already in UHV, whereas the introduction of a diluted H_2 atmosphere did not result in a further reduction of the residual oxygen concentration upon annealing, (*ii*) a significant increase of the Ni/Ga surface

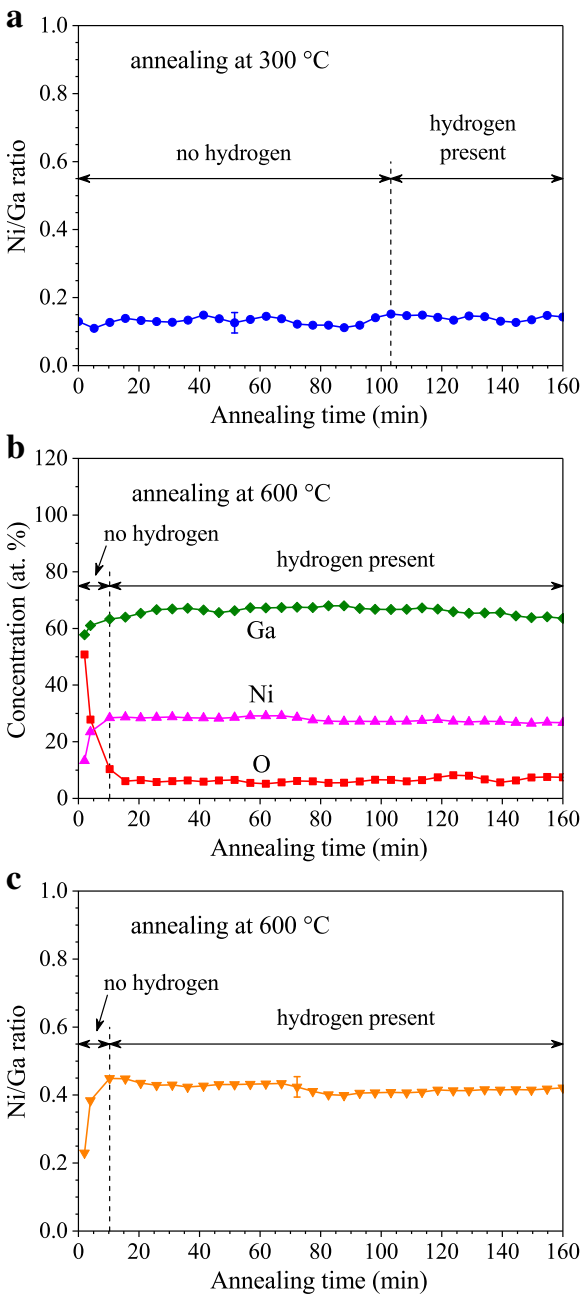

Fig. 6 **a** Time dependence of the Ni/Ga concentration ratio in the surface layer (3–5 nm depth) during annealing at 300 °C. **b** Time dependence of the O, Ga and Ni concentrations in the surface layer during annealing at 600 °C. **c** Time dependence of the Ni/Ga concentration ratio in the surface layer during annealing at 600 °C

concentration ratio has happened during the same initial period in UHV, so that the drop of the oxygen concentration is directly related to the increase of the nickel concentration at the surface, (*iii*) the starting $R^{surf}_{Ni/Ga} = 0.23$ value at 600 °C was a factor of about 2 larger than the corresponding value at 300 °C (and also at 25 °C) $R^{surf}_{Ni/Ga} = 0.12$, so that some enhancement of the nickel concentration at the surface has happened already during heating the material from 300 to 600 °C in UHV (that was accomplished in the time of 2 h).

4. In the fourth step, the crystal was cooled back to room temperature in UHV. The measurement of the elemental concentrations at 25 °C has shown that the Ni/Ga surface concentration ratio remained enhanced to the value $R^{surf}_{Ni/Ga} = 0.43$.

The type of chemical bonding of Ga at different depths in the concentration profile was determined by decomposing Ga XPS signal into the Ga-oxide and Ga-metallic signals. The high-resolution Ga $2p_{3/2}$ XPS spectra at several depths between the surface and 30 nm of the oxidized material at 25 °C (prior to the annealing experiments, corresponding to the depth profile of Fig. 5a) is shown in Fig. 7a. At the surface, Ga is fully oxidic, whereas at the depths larger than about of 10 nm, Ga is in the metallic form. The thickness of the surface gallium-oxide layer was consequently estimated as 6 ± 2 nm. The spectra at 25 °C after the completed annealing at 600 °C are shown in Fig. 7b. All Ga is metallic at any depth, including at the surface. This confirms that annealing at 600 °C has effectively cleaned the surface oxide.

The results for the chemical bonding of Ni obtained from high-resolution Ni $2p_{3/2}$ XPS spectra are analogous. No signal of metallic Ni could be observed within the surface layer of the oxidized material prior to the annealing (Fig. 7c), whereas metallic Ni is present at the surface after annealing at 600 °C (Fig. 7d).

Discussion

The XPS study of a monocrystalline surface has shown that the elemental composition of the Ga_3Ni_2 oxidized surface is strongly enhanced in Ga and depleted in Ni ($R^{surf}_{Ni/Ga} = 0.12$) relative to the concentrations of these elements in the bulk ($R^{bulk}_{Ni/Ga} = 0.83$) for the specific crystallographic orientation of the surface. Annealing at 600 °C has resulted in the oxide removal and partial reconstruction of the surface towards higher Ni concentration ($R^{surf}_{Ni/Ga} = 0.43$), whereas the annealing at 300 °C did not. The surface reconstruction at 600 °C has happened already in UHV within the time of about 12 min, whereas the subsequent introduction of a diluted H_2 reducing atmosphere and further annealing for 2 h did not change the surface concentrations of Ni and Ga anymore. This indicates that the oxide removal and the surface reconstruction process were already completed

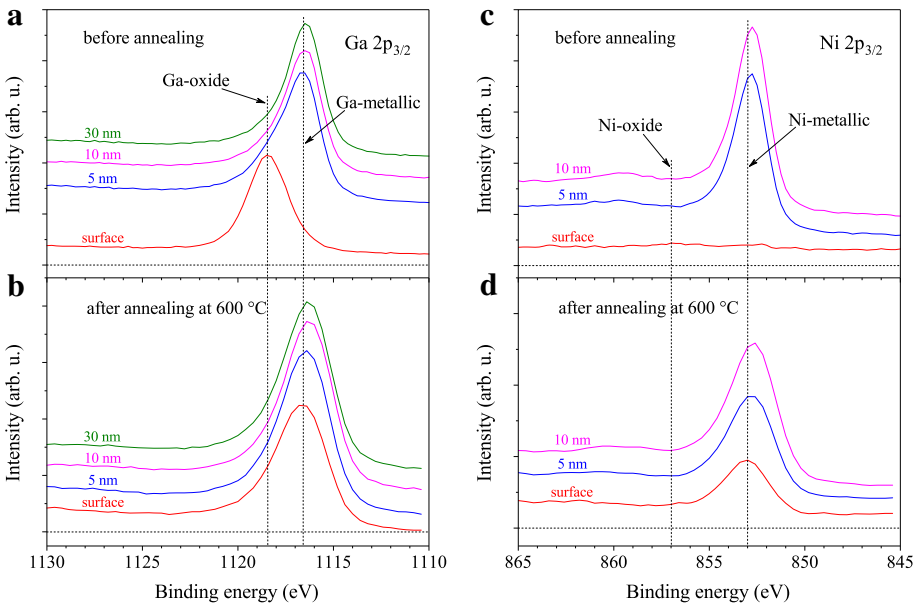

Fig. 7 Ga $2p_{3/2}$ XPS high-resolution spectra at several depths between the surface and 30 nm at 25 °C of **a** the Ga_3Ni_2 oxidized monocrystalline surface (prior to the annealing experiments) and **b** after annealing at 600 °C. The corresponding Ni $2p_{3/2}$ spectra of **c** the oxidized surface and **d** after annealing at 600 °C. The spectra are not normalized

during annealing in UHV, so that the effectiveness of the static diluted H_2 reducing atmosphere could not be assessed. After cooling back to room temperature in UHV, the Ni/Ga surface concentration ratio remained enhanced to the value $R^{surf}_{Ni/Ga} = 0.43$.

The above results can be understood by the following picture. Upon contact of the Ga_3Ni_2 material to the air, surface gallium oxide (very likely Ga_2O_3) and nickel oxide (NiO) are formed almost instantaneously. The standard enthalpy of formation of Ga_2O_3 ($\Delta H^0_f = -1089.1$ kJ/mol) (Haynes 2011) is a factor of 4.5 more negative than the one of NiO ($\Delta H^0_f = -240.0$ kJ/mol), so that higher affinity of Ga to oxygen pushes Ga to the surface, whereas Ni consequently sinks into the subsurface region. As a result, the concentration of Ga at the oxidized surface is strongly enhanced and the concentration of Ni is strongly depleted with respect to the values in the bulk. By annealing the surface at 600 °C in UHV, the oxides evaporate (Ga_2O_3 decomposes into volatile lower oxides and oxygen (Stepanov et al. 2016)) and thermal diffusion of atoms near the surface partially reconstructs the surface composition towards the energetically more favorable bulk value. Since the standard enthalpy of formation of Ga_3Ni_2 is $\Delta H^0_f = -45$ kJ/mol (de Boer et al. 1988), more nickel at the surface reduces the energy. By annealing the surface at a lower temperature of 300 °C, thermal energy of the atoms is too small to remove the oxides in UHV, whereas the H_2 reducing atmosphere appears to be too diluted to be effective in cleaning the oxides (the H_2 gas could be filled into the UHV chamber to a maximum pressure of 10^{-7} mbar only, in order that the XPS instrument was still operating).

In the CO_2 catalytic conversion experiments, the experimental conditions were different from those in the XPS. There was no UHV but the pressure was close to atmospheric, whereas the density of the H_2 reducing atmosphere was high. Reduction with H_2 flowing gas has effectively cleaned the surface oxides at both 300 and 600 °C. The subsequent reconstruction of the oxide-free surface by atomic diffusion towards higher Ni concentration has proceeded in the same way as in the XPS experiments. The Ni/Ga surface concentration ratio depended on the temperature and on the time spent at that temperature. The increased CO_2 conversion of the catalyst reduced at 600 °C with respect to the 300 °C-reduced one (Fig. 3a) is a consequence of the increased Ni concentration at the surface. This is supported by the fact that the amounts of released H_2 and CO in the TPD experiments, the metal dispersion D and the reaction rate r_{CO_2} for the 600 °C-reduced catalyst all increase by the same factor of about 1.7 with respect to the 300 °C reduction, whereas the TOF (representing the CO_2 conversion per single active site) is the same for both reduction temperatures. These results, together with the XPS analysis, confirm that nickel is the catalytically active species of the Ga_3Ni_2 catalyst. Microscopic identification of the active sites (coordination of Ni by Ga atoms and/or by other Ni atoms) cannot be inferred from our experiments.

Conclusions

In a routine handling of the catalyst material, exposure to air can usually not be avoided. For noble metal catalysts that are resistant to oxidation, this is not an issue, but becomes important for intermetallic catalysts composed of two or more non-noble chemical elements that possess much different standard enthalpies of the oxide formation. The element with higher affinity to oxygen (more negative standard enthalpy of formation) concentrates on the surface in the oxide form, whereas the element with lower affinity sinks into the subsurface region. The surface stoichiometry may thus be strongly altered with respect to the bulk one, which affects the number of active sites at the surface and the catalytic performance. We have investigated the instability of the active surface chemical composition to oxidation for the Ga_3Ni_2 intermetallic catalyst, a new catalyst for the CO_2 reduction from the Ga–Ni phase diagram that has not been investigated previously. XPS study of the surface subjected to different heating–annealing conditions has shown that the concentration of Ga at the oxidized surface is strongly enhanced and the concentration of Ni is strongly depleted with respect to the values in the bulk, because of a 4.5 times more negative standard enthalpy of formation of Ga_2O_3 relative to NiO. By annealing the surface at 600 °C in UHV, the oxides have evaporated and thermal diffusion of atoms near the surface has partially reconstructed the surface composition towards the energetically more favorable bulk value. By annealing the surface at a lower temperature of 300 °C, thermal energy of the atoms was too small to remove the oxides in UHV and the surface reconstruction did not take place.

In the CO_2 conversion experiments, the reduction with H_2 gas prior to the catalytic tests has effectively cleaned the surface oxides for both, 300 or 600 °C reduction temperatures. The subsequent reconstruction of the oxide-free surface by atomic diffusion towards higher Ni concentration has proceeded in the same way as in the XPS experiments. The Ni/Ga surface concentration ratio depended on the temperature and the time spent at that temperature. A significantly increased CO_2 conversion (by a factor 1.7) of the catalyst reduced at 600 °C, with respect to the 300 °C-reduced one was detected, as a consequence of the increased Ni concentration at the surface by the same factor.

The instability of the active surface chemical composition to oxidation in air must be taken into account when considering noble metal-free intermetallic catalysts as alternatives to the conventional catalysts based on noble metals. Ga_3Ni_2 and other Ga–Ni intermetallic compounds are good examples of binary intermetallic catalysts, whose catalytic performance is strongly affected by exposure to the air.

Acknowledgements
We thank Prof. Marc Armbrüster from TU Chemnitz for fruitful discussions.

Funding
Slovenian authors acknowledge the financial support from the Slovenian Research Agency (research core funding No. P1–0125). MW is grateful for funding by the German Academic Exchange Service (DAAD), Grant no. A/14/02942.

Availability of data and materials
The data used in this study is presented in the main paper. Request for material to JD.

Authors' contributions
MW and PG synthesized the catalysts material. AJ and SV performed characterization of the material. VDBCD and BL conducted catalytic testing. JK performed surface analysis by XPS. HJK contributed analysis of catalytic results. JD has coordinated the work and wrote the paper. All authors read and approved the final manuscript.

Competing interests
The authors declare that they have no competing interests.

Publisher's Note

Author details
[1]Institute of Molecular Physics, Polish Academy of Sciences, Smoluchowskiego 17, 60-179 Poznań, Poland. [2]Jožef Stefan Institute, Jamova 39, 1000 Ljubljana, Slovenia. [3]Department of Catalysis and Chemical Reaction Engineering, National Institute of Chemistry, Hajdrihova 19, 1000 Ljubljana, Slovenia. [4]Department of Earth and Environmental Sciences, Crystallography Section, Ludwig-Maximilians-Universität München, Theresienstraße 41, 80333 Munich, Germany. [5]Division of Material Science Research, Korea Basic Science Institute, Daejeon 305-333, Republic of Korea. [6]Faculty of Mathematics and Physics, University of Ljubljana, Jadranska 19, 1000 Ljubljana, Slovenia.

Received: 25 April 2018 Accepted: 31 May 2018
Published online: 11 June 2018

References

Armbrüster M, Kovnir K, Behrens M, Teschner D, Grin Y, Schlögl R. Pd–Ga intermetallic compounds as highly selective semihydrogenation catalysts. J Am Chem Soc. 2010;132:14745–7.
Armbrüster M, Kovnir K, Friedrich M, Teschner D, Wowsnick G, Hahne M, Gille P, Szentmiklósi L, Feuerbacher M, Heggen M, Girgsdies F, Rosenthal D, Schlögl R, Yu G. $Al_{13}Fe_4$ as a low-cost alternative for palladium in heterogeneous hydrogenation. Nat Mater. 2012;11:690–3.
Armbrüster M, Kovnir K, Grin Y, Schlögl R. Complex metallic phases in catalysis. In: Dubois JM, Belin-Ferré E, editors. Complex metallic alloys: Fundamentals and Applications. Weinheim: Wiley–VCH; 2011. p. 385–99.
Armbrüster M, Schlögl R, Yu G. Intermetallic compounds in heterogeneous catalysis—a quickly developing field. Sci Technol Adv Mater. 2014;15:034803.
de Boer FR, Boom R, Mattens WCM, Miedema AR, Niessen AK. Cohesion in metals: transition metal alloys (cohesion and structure). Amsterdam: North Holland; 1988.
Haynes WM. CRC Handbook of chemistry and physics. 92nd ed. Boca Raton: CRC Press; 2011.
Hellner E, Laves F. Crystal chemistry of indium and gallium in alloys with some transition elements (Ni, Pd, Pt, Cu, Ag, and Au). Z Naturforschung. 1947;2a:177–83.
Kim SS, Lee HH, Hong SC. The effect of the morphological characteristics of TiO_2 supports on the reverse water–gas shift reaction over Pt/TiO_2 catalysts. Appl Catal B Environ. 2012;119–120:100–8.
Kim SS, Park KH, Hong SC. A study of the selectivity of the reverse water–gas-shift reaction over Pt/TiO_2 catalysts. Fuel Process Technol. 2013;108:47–54.
Klanjšek M, Gradišek A, Kocjan A, Bobnar M, Jeglič P, Wencka M, Jagličić Z, Popčević P, Ivkov J, Smontara A, Gille P, Armbrüster M, Grin Y, Dolinšek J. PdGa intermetallic hydrogenation catalyst: an NMR and physical property study. J Phys Condens Matter. 2012;24:085703.
Kovnir K, Armbrüster M, Teschner D, Venkov TV, Jentoft FC, Knop–Gericke A, Yu G, Schlögl R. A new approach to well-defined, stable and site-isolated catalysts. Sci Technol Adv Mater. 2007;8:420–7.
Okamoto H. Ga-Ni (Gallium-Nickel). J Phase Equil Diffus. 2010;31:575–6.
Osswald J, Giedigkeit R, Jentoft RE, Armbrüster M, Girgsdies F, Kovnir K, Grin Y, Schlögl R, Ressler T. Palladium–gallium intermetallic compounds for the selective hydrogenation of acetylene: part I: preparation and structural investigation under reaction conditions. J Catal. 2008;258:210–8.
Sharafutdinov I, Elkjær CF, de Carvalho HWP, Gardini D, Chiarello GL, Damsgaard CD, Wagner JB, Grunwaldt J–D, Dahl S, Chorkendorff I. Intermetallic compounds of Ni and Ga as catalysts for the synthesis of methanol. J Catal. 2014;320:77–88.
Stepanov SI, Nikolaev VI, Bougrov VE, Romanov AE. Gallium oxide: properties and applications—a review. Rev Adv Mater Sci. 2016;44:63–86.
Studt F, Sharafutdinov I, Abild-Pedersen F, Elkjær CF, Hummelshøj JS, Dahl S, Chorkendorff I, Nørskov JK. Discovery of a Ni-Ga catalyst for carbon dioxide reduction to methanol. Nat Chem. 2014;6:320–42.
Wencka M, Hahne M, Kocjan A, Vrtnik S, Koželj P, Korže D, Jagličić Z, Sorić M, Popčević P, Ivkov J, Smontara A, Gille P, Jurga S, Tomeš P, Paschen S, Ormeci A, Armbrüster M, Grin Y, Dolinšek J. Physical properties of the InPd intermetallic catalyst. Intermetallics. 2014;55:56–65.
Wencka M, Pillaca M, Gille P. Single crystal growth of Ga_3Ni_2 by the Czochralski method. J Cryst Growth. 2016;449:114–8.
Wencka M, Schwerin J, Klanjšek M, Krnel M, Vrtnik M, Koželj P, Jelen A, Kapun G, Jagličić Z, Sharafutdinov I, Chorkendorff I, Gille P, Dolinšek J. Physical properties of the $GaPd_2$ intermetallic catalyst in bulk and nanoparticle morphology. Intermetallics. 2015;67:35–46.